(COSY Proposal and Beam Request #172.1)

Measurement of the $\vec{d}\vec{p} \to \{pp\}\, n$ Charge–Exchange Reaction with Polarised Beam and Target

A. Garishvili, A. Kacharava, A. Nass, A. Mussgiller, E. Steffens
Physikalisches Institut II, Universität Erlangen–Nürnberg, 91058 Erlangen, Germany

V.V. Glagolev
Joint Institute for Nuclear Research, Laboratory of High Energy, 141980 Dubna, Russia

D. Chiladze, A. Dzyuba, R. Engels, R. Gebel, K. Grigoryev, M. Hartmann, V. Hejny, I. Keshelashvili, B. Lorentz, M. Mikirtytchiants, M. Nekipelov, D. Oellers, H. Ohm, D. Prasuhn, F. Rathmann, R. Schleichert, H. Seyfarth, H.J. Stein, H. Ströher, Yu. Valdau
Institut für Kernphysik, Forschungszentrum Jülich, 52425 Jülich, Germany

S. Dymov, D. Gusev, V. Komarov, A. Kulikov, V. Kurbatov, V. Leontiev, G. Macharashvili, S. Merzliakov, V. Serdjuk, S. Trusov, Yu. Uzikov
Joint Institute for Nuclear Research, LNP, 141980 Dubna, Russia

B. Chiladze, D. Iamanidze, N. Lomidze, M. Nioradze, M. Tabidze
High Energy Physics Institute, Tbilisi State University, 0186 Tbilisi, Georgia

A. Khoukaz, T. Mersmann, M. Mielke, M. Papenbrock, T. Rausmann
Institut für Kernphysik, Universität Münster, 48149 Münster, Germany

S. Barsov, V. Koptev, S. Mikirtytchiants, A. Vasilyev
High Energy Physics Department, Petersburg Nuclear Physics Institute, 188350 Gatchina, Russia

L. Barion, P. Lenisa
University of Ferrara and INFN, 44100 Ferrara, Italy

J. Carbonell
Laboratoire de Physique Subatomique et de Cosmologie, 38026 Grenoble Cedex, France

C. Wilkin
Physics and Astronomy Department, UCL, London WC1E 6BT, U.K.

for the ANKE Collaboration

Jülich, March 2007

Abstract

The **one week** granted for the measurement of the $\vec{d}\vec{p} \to (pp)n$ deuteron charge–exchange reaction was taken in January 2007. The results of this have shown that we can investigate successfully reactions with a polarised deuteron beam and polarised hydrogen storage cell target. In particular, we have proved that we can calibrate the target polarisation by employing well identified nuclear reactions together with the Lamb–Shift Polarimetry (LSP) measurements. Furthermore, we have shown that we can handle the vector and tensor polarisations of the COSY beam. Since the necessary equipment has already been commissioned, it is now time to advance our programme by proposing production runs using a polarised hydrogen storage cell target in conjunction with a polarised deuteron beam.

At low excitation energies E_{pp} of the final pp system, the spin observables are directly related to the spin–dependent parts of the neutron–proton charge–exchange amplitudes. Our measurement of the deuteron–proton spin correlations will allow us to determine the relative phases of these amplitudes in addition to their overall magnitudes. This was the primary aim of our proposal #172.0, which was already discussed in length at PAC session #32. The proposal required in TOTAL **four weeks** of beam time to determine the vector $C_{y,y}(C_{x,x})$ and tensor $C_{yy,y}$ spin–correlation coefficients at two energies $T_d = 1.2\,\mathrm{GeV}$ and $T_d = 2.23\,\mathrm{GeV}$.

In the framework of the PRESENT document, based on the experience from our first test measurements, the collaboration asks for the allocation of **four weeks** of beam time to complete the proposed experiment after the reinstallation of the Polarised Internal Target (PIT) at ANKE.

Contents

1 Executive Summary

The data analysis of the measurements from the **ONE week** of beam time with a 1.2 GeV energy polarised deuteron beam incident on a polarised hydrogen storage cell target, taken in January 2007 at ANKE, is still far from being complete. Nevertheless, we have achieved the following:

- For the first time, studies with the COSY polarised deuteron beam were performed using a storage cell [25 μm aluminium foil, with the inner surface covered by Teflon, of 20 $\times$ 15 mm^2 cross section and 390 mm length]. For this purpose the machine group furnished a polarised deuteron beam, electron cooled, stacked at injection and accelerated to T_d=1.2 GeV (P_d=2.435 GeV/c);

- To improve the COSY beam intensity, a longer stacking injection was implemented. In double–polarised measurements we worked with a cycle of 45(50) minutes duration: 15(20) minutes for stacking (90(120) stacks separated by 10 s for cooling) and 30 minutes for the flat top. Under these conditions 7×10^9 polarised deuterons were accelerated to the flat–top energy of 1.2 GeV;

- It has been shown that the procedure of scraping the accelerated beam before the data–taking minimised the background events coming from the interactions of the beam halo particles with the cell wall. Even without using stochastic cooling (this is not possible at COSY at the beam energy of $T_d = 1.2$ GeV), the achieved beam quality generally allowed the deuterons to pass through the cell without touching the walls;

- The expected density for the polarised hydrogen ($\vec{\mathrm{H}}$ gas) storage cell target of $d_t = 1.34 \times 10^{13}\,\mathrm{cm}^{-2}$ was achieved. This value, together with the beam intensity of 7×10^9 stored polarised deuterons, led to a luminosity of $L = 1.0 \times 10^{29}\,\mathrm{s}^{-1}\mathrm{cm}^{-2}$;

- In parallel to the data–taking, the ABS source has been tuned with Lamb–shift Polarimeter (LSP) measurements. The goal was to determine the target polarisation (Q_y) from the quasi–free $\boldsymbol{n\vec{p} \to d\pi^0}$ reaction. The achieved value of average target polarisation of $\langle Q_y \rangle = 0.75 \pm 0.06$, is much higher then it was in the the first measurements in 2006. Thus, the target polarisation has been maximised and the equality of positive and negative polarisations has been verified on the level of a couple of percent by using on–line measurements from the LSP, repeated every 24 hours;

- The clean identification of events for the $\boldsymbol{\vec{d}\vec{p}}$–induced reactions when using a long cell target has been demonstrated. This was done on the basis of experimental information obtained from the $\vec{\mathrm{H}}$ gas target and on the known shape of the background from the cell walls, which is imitated through the use of N_2 gas in the cell. The exact shape of the background under the missing–mass peak from the cell–wall events has been determined under real experimental conditions and was under control during on-line measurements;

- Using the missing–mass technique for the measured single– and double–track events in ANKE, it has been shown that very clean identification of the following reactions is possible: $\boldsymbol{\vec{d}\vec{p} \to dp_{sp}\pi^0}$ (both branches of quasi–free $\boldsymbol{\vec{n}\vec{p} \to d\pi^0}$), $\boldsymbol{\vec{d}\vec{p} \to (pp)n}$, $\boldsymbol{\vec{d}\vec{p} \to {}^3\mathrm{He}\,\pi^0}$, and $\boldsymbol{\vec{d}\vec{p} \to dp}$. The last channel was identified unambiguously with very little background by using silicon detectors in coincidence with the forward detector system;

- Differential distributions for the $\vec{\boldsymbol{d}}\vec{\boldsymbol{p}} \rightarrow (\boldsymbol{pp})\boldsymbol{n}$ reaction have been obtained as functions of the momentum transfer t and the pp excitation energy E_{pp};

- We have worked with five different combinations of vector (P_z) and tensor (P_{zz}) deuteron polarisations provided by the ion source and accelerated in COSY. At the beginning of data–taking, the Low Energy Polarimetry (LEP) measurements were done with eight different combinations of P_z and P_{zz} and, based on these results, the five best spin modes were selected;

- We have extracted the value of the deuteron beam vector polarisation P_z from the quasi–free $\vec{\boldsymbol{n}}\boldsymbol{p} \rightarrow \boldsymbol{d}\boldsymbol{\pi}^{\boldsymbol{0}}$ reaction using the angular dependence of the analysing power of the $\vec{\boldsymbol{p}}\boldsymbol{p} \rightarrow \boldsymbol{d}\boldsymbol{\pi}^{+}$ reaction, which was also used determine the target polarisation. The result, $\langle P_z^{ANKE} \rangle = 0.60 \pm 0.10$, is compatible with the value of $\langle P_z^{LEP} \rangle = 0.660 \pm 0.003$, obtained from the LEP measurements.

The January 2007 data have to be further studied in order to:

- Determine the values of P_z and P_{zz} of the beam from the $\vec{d}\vec{p} \rightarrow dp$ elastic scattering data, and compare P_z value with the one obtained from the quasi–free $\vec{\boldsymbol{n}}\boldsymbol{p} \rightarrow \boldsymbol{d}\boldsymbol{\pi}^{\boldsymbol{0}}$ reaction;

- Cross check the above described methods by comparing the results with the polarisation obtained from the pp quasi–elastic process, which will be identified with the silicon–telescope system;

- Reconstruct the extended cell–target vertex coordinates using the method which has been applied successfully to the data obtained with the proton beam;

- Obtain the target polarisation dependence as a function of the vertex coordinate (Z) along the cell to evaluate depolarisatiion effects on the cell walls;

- Investigate the effects of the data cuts on the extraction of the polarisation observables with the aim of reducing down to the level of the statistics the variations apparent for the different spin modes.

Given the above successes in the <u>first</u> handling of the double–polarised measurements at COSY, we request **four weeks** of beam time to determine the vector $C_{y,y}, (C_{x,x})$ and tensor $C_{yy,y}$ spin correlation coefficients at two energies $T_d = 1.2\,\mathrm{GeV}$ and $T_d = 2.23\,\mathrm{GeV}$, and complete the proposed experiment at both energies in early 2008, after the reinstallation of the PIT at ANKE.

In the following pages we attempt to justify the statements made in the above summary.

2 Introduction

In autumn 2006 we submitted to the PAC session No. 32 a proposal (#172), where we aimed to study the $\vec{d}\vec{p} \to \{pp\}\, n$ Charge–Exchange (CE) reaction with a polarised beam and target at two momenta, 2.4 GeV/c and 3.7 GeV/c [1]. The purpose is to determine the vector $C_{y,y}, (C_{x,x})$ and tensor $C_{yy,y}$ spin–correlation coefficients in the kinematical region of low excitation energy in the final proton–proton system. The interpretation of the results is simplified here since it can be shown that the spin observables are, to a good approximation, directly related to the spin–dependent parts of the CE amplitudes in this region. This will allow the determination of the relative phases between amplitudes. Such data are of importance for the phase shift analysis of the *np* system where data are scarce. Concerning this work it was stated in the PAC recommendations: *This proposal concerns the first double–polarisation experiment at COSY. The PAC has already expressed the importance of such measurements at ANKE for coming years and encourages this measurements. However, two questions concerning the feasibility of the proposed experiment (#172) were discussed and require further clarification before the full 4 weeks of requested beam time can be granted. One question concerns the shape of the background under the missing–mass peak. The exact shape of the background from the cell walls under real experimental conditions with a deuteron beam will be studied in pilot measurements during the PIT and STT commissioning early 2007. Another question concerns the target polarisation. The average polarisation should be maximised and the equality of positive and negative polarisation should be verified. The collaboration expressed interest to solve these questions before the production run. The PAC recommends* **one week** *of beam time in the coming period for the optimisation of the target polarisation. The approval of the remaining three weeks will depend on the results from the PIT, STT and target commissioning.* This **one week** of beam time for the experiment #172 was taken in January 2007 and the results from this run, together with an updated beam request for **four weeks** of beam time, are presented in the current document.

3 Schedule of the January beam time activities

The polarised internal target (PIT) system at ANKE consists of an atomic beam source (ABS) feeding a storage cell (SC) and a Lamb–shift polarimeter (LSP). For commissioning of the PIT (experiment #146.2 [2]) the PAC in session No. 31 approved **one week of machine development and one week of beam time**. In the same session, the PAC also recommended to share this time for testing the Silicon Tracking Telescope (STT) system (experiment #159 [3]) in the new PIT environment.

These commissioning efforts were undertaken in January 2007 in the following time sequence:

1. **Machine development week, January 8–14**: COSY beam studies were performed using a storage cell, produced from 25 μm Al foil with the inner surface covered by Teflon. The size was 20×15 mm^2 cross section, 390 mm length (in the following given as $20 \times 15 \times 390$ mm^3). For this purpose the machine group started by using an unpolarised deuteron beam, electron cooled, stacked at injection and accelerated to T_d=1.2 GeV (P_d=2.435 GeV/c). ANKE was first positioned at 0° (beam straight through) to set up the E–cooler, and the beam then accelerated with the cell in place. After this, ANKE was moved to 5.5° and the procedure repeated. During the weekend, data were taken with the ANKE forward detector using the unpolarised deuteron beam and polarised hydrogen atomic beam $\vec{\mathrm{H}}$ injected into the

cell. In parallel to the data–taking, the transition units in the ABS were tuned using the LSP. The goal was to determine the target polarisation (Q_y) from the quasi–free $\boldsymbol{n\vec{p} \to d\pi^0}$ reaction. The achieved results are given in section 4.5.

2. **PIT & STT commissioning week, January 15–21**: At the beginning of this week the polarised source was set up and Low Energy Polarimetry (LEP) measurements behind the cyclotron were performed. The optimisation of the stacking procedure of the polarised deuteron beam into COSY was then started with the aim of achieving the highest possible beam intensity. During three days data were taken with a polarised deuteron beam and unpolarised H_2 target from the unpolarised Gas Supply System (UGSS) with the calibrated flux admitted into the cell. The goal was to determine the vector polarisation (P_z) of the deuteron beam from the same quasi–free $\boldsymbol{\vec{n}p \to d\pi^0}$ reaction. The achieved results are to be found in section 4.7.

   The rest of the week was used for the silicon tracking telescope (STT) installation and commissioning. Unfortunately, because of hurricane 'Kirill', we were forced to start the beam development with the polarised COSY beam again and to repeat the LEP measurements. The main purpose of this week was to show that the silicon detectors can operate under PIT conditions with cooled and stacked beam through the storage cell at injection. At the end of the week we took some data for STT commissioning. The achieved results are reported in section 4.4.4.

3. **Data–taking in the double–polarised mode, January 22–29**: At the beginning of this week, using scrapers for the polarised COSY beam, the conditions for STT operation close to the PIT storage cell were optimised. We subsequently collected data on several nuclear reactions from the double–polarised measurements with ANKE, including the STT. In parallel to the usual data–taking, LSP measurements were performed every 24 hours in order to check the stability of the transition units in the ABS. Also, a few runs were taken with the unpolarised H_2 target to determine the cell target density from Schottky spectra (see section 4.2) and with the unpolarised N_2 target to identify the shape of the 'background' events from the storage cell walls.

4 Achieved results

4.1 COSY–beam intensities with storage cell

In the first beam–time session, the unpolarised deuteron beam and polarised hydrogen storage cell target were used. To achieve the maximum COSY–beam intensity with the storage cell, a couple of days were spent tuning the beam, first without and afterwards with the cell in the beam. With ANKE positioned at 5.5°, about 9×10^9 unpolarised deuterons were accelerated in the ring to pass through the polarised hydrogen gas in the cell. The intensity achieved could be increased when no gas was injected into the storage cell during stacking (empty cell).

For the second beam–time session, COSY was switched to polarised deuterons. Optimisation of the stacking procedure (about 90 stacks separated by 2 s for cooling) of the polarised deuteron beam in COSY was then started and the acceleration of about 2.5×10^9 polarised deuterons has been achieved on flat top with a cycle duration of 600 s.

For the third part of the beam–time, a longer stacking injection was implemented to improve the COSY intensity. After some optimisation between the accelerated beam intensity and the ratio of unused (at injection) and used (on flat top) time, we worked with

a cycle of 45 min duration: 15 min stacking (90 stacks separated by 10 s for cooling) and 30 min flat top. Such a cycle is shown in Fig. 1 by the red curve. Under these conditions 7×10^9 polarised deuterons were accelerated to the energy of 1200 MeV. The higher beam intensity was possible only due to the long injection and flat top time. In addition to this procedure, the scraping of the accelerated beam on flat top just before the data taking allowed us to minimise the background events from the interactions of the beam halo particles on the cell wall.

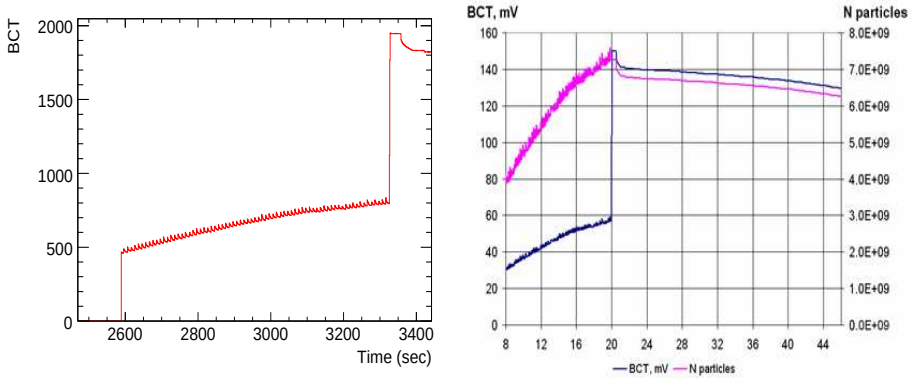

Figure 1: Left panel: characteristic cycle with 90 injected stacks, each followed by 10 s electron cooling. Right panel: characteristic cycle after acceleration for 1800 s flat top. The number of stored particles is deduced from the voltage signal of the Beam-Current-Transformer (BCT).

4.2 Storage cell target density

During the beam time a new storage cell, built from 25 μm Al foil with the inner surface covered by Teflon, was used. It has a rectangular cross–section of $20 \times 15\,\mathrm{mm}^2$, in horizontal and vertical direction respectively, and 390 mm length, with rounded corners of 2 mm radius (in the following given as $20 \times 15 \times 390\,\mathrm{mm}^3$). Thus, it gives the same cross–sectional area for the beam tube as a circular tube of 19.43 mm diameter. The ABS gas feeding tube was positioned 35 mm off the centre of the COSY–beam tube. For this assembly, calculations based on the ABS–flux calibration with the Unpolarised Gas Supply System (UGSS) were carried out. A picture of the cell, taken before and after its installation in the target chamber, is shown in Fig. 2.

The idea of these calibrations is to measure a pushing pressure in the UGSS volume and the pressure in the compression tube setup at the interaction point of the ABS and the COSY beams as functions of time. By observing the time dependence of the decay of the pressure it is possible to calculate the flux into the compression tube as a function of the pressure in the UGSS. Knowing the pressure in the compression tube when the ABS is used, it is possible to calculate the flux into the storage cell (in atoms per second).

Since the gas type is known, it is very simple to calculate the pressure in the centre of the storage cell and, based on the geometry, also the linear target density. The pressure is highest at the position of the feeding tube centre and goes to zero at the entrance and exit of the beam tube. The conductance of the beam tube is the sum of the conductances of the two halves and can be calculated with use of the formulae [4]: $C_{tube}(M, d, L) = \sqrt{T/M} \times 2.85 \times 10^{-2}\, d^3/(d + 0.75L)$, where M is atomic mass number, T the gas temperature (K), d and L are the diameter (mm) and length (mm) of the tubes, respectively.

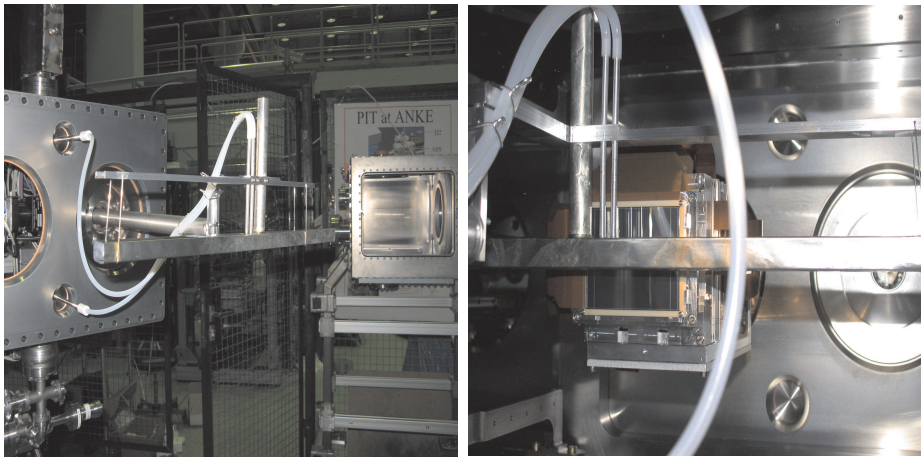

Figure 2: Left panel: the storage cell before its installation in the ANKE target chamber. Right panel: storage cell installed in the target chamber together with Silicon Tracking Telescope (STT) system, which is seen in the picture behind the cell.

It was found that the pressure of molecular hydrogen in the UGSS volume of 450 mbar gives slightly higher pressure in the storage cell compare to the full ABS flux (2 HFS of the hydrogen). The expected total areal target density with the present cell design is $d_t = 2.68 \times 10^{13}$ [atoms/cm^2].

However, this is not the only method to determine a target thickness. It is possible to measure the deceleration of the beam in the storage ring during the cycle. The Schottky spectra during the individual cycle show the beam deceleration after passing the target, which gives the shift in the revolution frequency of the beam. This shift depends on the target density and the type of gas in the target.

4.3 Installation of the Lamb–Shift Polarimeter and measurements with the ABS

The use of the Lamb–shift Polarimeter (LSP) at the ANKE target position for the tuning of the rf–transition units and measuring the polarisation of the atomic beam from the ABS injected into the LSP was one of the primary goals of the PIT commissioning during the January 2007 beam time. This already allowed a polarisation measurement of the direct ABS beam and thus enabled on–line tuning of the rf–transition units in the laboratory [5]. Preliminary results of the nuclear polarisation in the laboratory demonstrated the feasibility of the method. The sensitivity, however, had to be enhanced substantially in order to achieve the envisaged accuracy. Therefore, it was planned for the January 2007 beam time to use the LSP in a modified geometry. The complete setup has been implemented below the ANKE target chamber (see Fig. 3) in the December 2006 shutdown period.

In this configuration about 30% of the total ABS flux after passing the ANKE target chamber is injected into the LSP. Another 70% of the beam is de-focused and pumped away by the additional Cryo–pump, which was installed in the target chamber to improve the vacuum conditions. The ABS beam in the LSP passes through the region of a strong magnetic field of the ioniser, mounted below the ANKE target chamber. The protons, produced in the ioniser, are deflected into the horizontal LSP beam line. The residual atoms are pumped away by a NEG (Non–Evaporable Getter) pump around the ionising volume, and a turbo pump in the deflector chamber. After the rotation of the quantisation

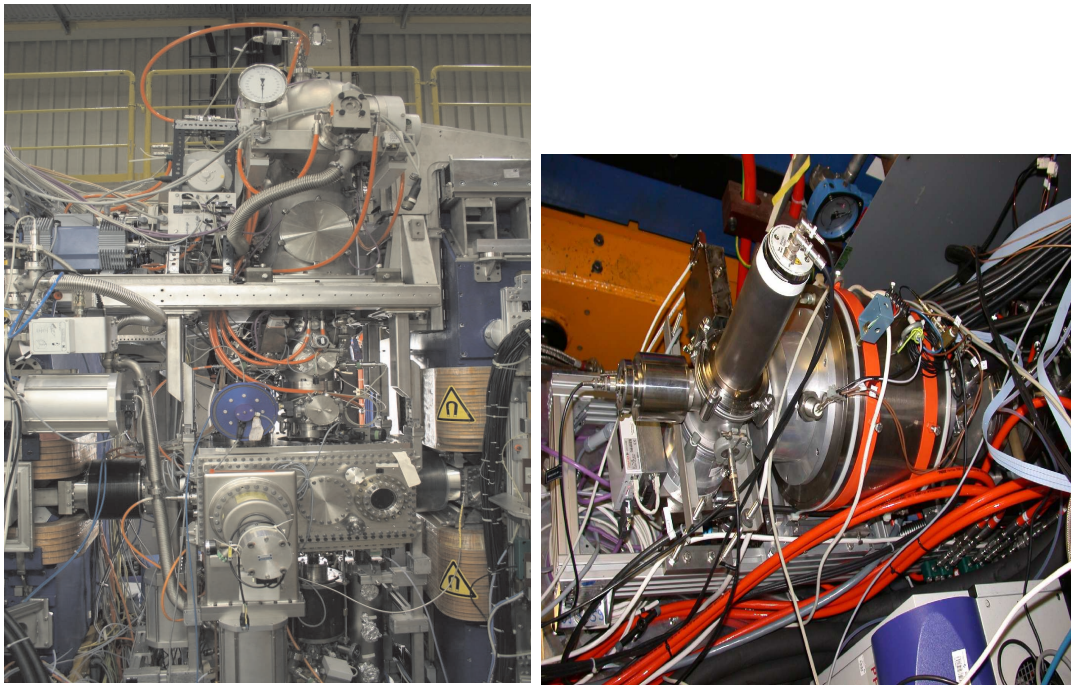

Figure 3: Left panel: the PIT (ABS+LSP) installation at the ANKE position. Right panel: from left to right the visible LSP components are the Faraday cup, the quenching chamber with the photomultiplier, the spin filter and the Cs cell. The Wien filter, the 90°–deflector and the ioniser are not visible.

axis by a Wien filter, the polarisation is measured with a combination of a Cs cell, a spin filter and a quenching region of the LSP [6].

During the December 2006 shutdown, the LSP was tested together with the ANKE central magnet D2 set to the magnetic fields foreseen for the January 2007 beam time. The asymmetries in the peaks of the Lyman–α spectrum, measured in the quenching chamber of the LSP, which are used to calculate the polarisation of the ABS jet, were about three times smaller than expected (see Fig. 4). The LSP measures the projection of the polarisation on the horizontal beam line. The stray fields of the D2 magnet produce a Larmor precession of the quantisation axis, which is very sensitive to the D2 fields. With some shielding around the Wien filter this effect has been stabilised and finally the angle between the polarisation and the beam line was around 160°. This effect can only be partially compensated with the actual Wien filter. Nevertheless, the measured asymmetries in the Lamb–shift spectra are proportional to the polarisation of the ABS atomic hydrogen beam.

The relative tuning of the transition units of the ABS was possible with an error of about 1%. It has been demonstrated that, with a new modified shielding for the weak field transition unit, its magnetic fields are not influenced by the D2 stray fields. Therefore the polarisation of the ABS hydrogen beam should to be switched between the maximum positive ($Q_y^+ = +0.898 \pm 0.004$) and negative values ($Q_y^- = -0.900 \pm 0.005$) [6]. In parallel to the usual data taking (session 3), the LSP measurements have been repeated every 24 hours in order to check the stability of ABS operation. These results are presented in Fig. 5.

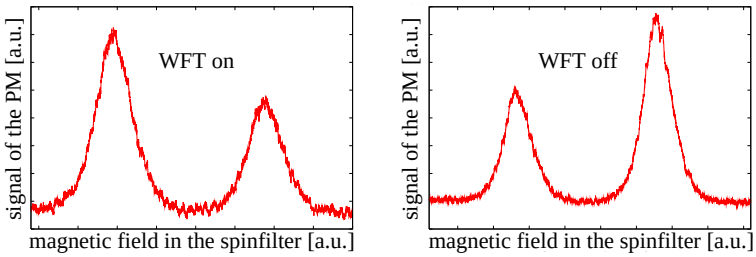

Figure 4: Asymmetries in the peaks of the Lyman–α spectrum measured in the quenching chamber of the LSP, when the weak field transition unit (WFT) was switched **on** (left spectra) and **off** (right spectra).

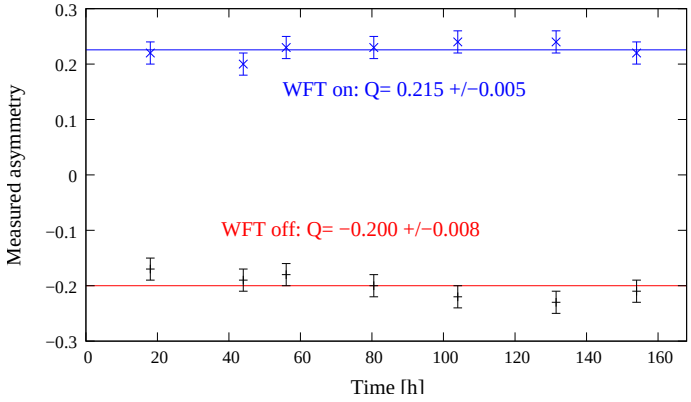

Figure 5: On–line measurements of the Lyman–α peak asymmetry from the LSP during the beam time from January 23 to 29, 2007.

4.4 Identification of nuclear reactions under PIT conditions

In this section the event identification for the dp–induced reactions are demonstrated when using a long cell target. This is done on the basis of experimental information obtained in dp interactions, especially from the shape of the background from the cell walls, which is imitated through the use of N_2 gas in the cell.

Figure 6 shows events where two charged particles were detected in the double–layer forward scintillation hodoscope during the January beam–time. Polarised $\vec{H}$ (Unpolarised N_2) gas was used in the cell with an incident deuteron beam energy of 1200 MeV. The figure shows the arrival–time differences for the two particles in the hodoscope (calculated after momentum and trajectory reconstruction under the assumption that both particles were protons) *versus* the measured difference of the two time signals from the scintillators. Thus, the two protons from the $dp \rightarrow (pp)n$ reaction should lie along the diagonal, with other particle pairs (such as dp) being found elsewhere. The off–diagonal events are, of course, mirrored about the diagonal. A similar picture was obtained with the H_2 cluster target measurements [7].

Reactions in the N_2 gas in the cell are expected to show similar smearing of the ejectile momenta due the Fermi motion of the nucleons as reactions in the aluminium cell–wall material [8]. The comparison of the results presented in the two panels of Fig. 6 in fact show strong effects for both pp and $dp\pi^0$ events. This should allow one to discriminate between reactions with the $\vec{H}$ (and later also $\vec{D}$) gas in the storage cell from wall events due to the different widths in the momentum distribution. On the other hand, the narrow

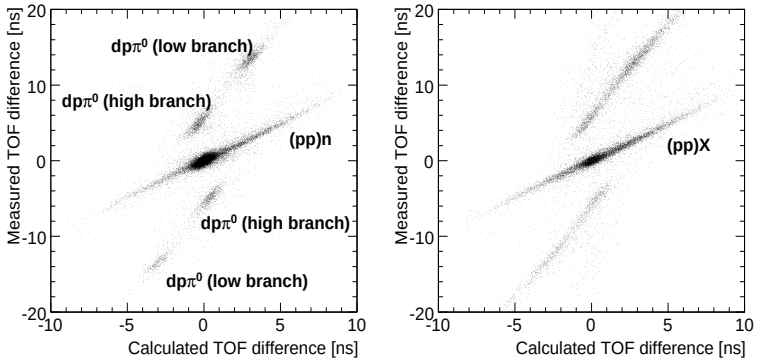

Figure 6: Time difference of the two detected charged particles, calculated under the assumption that both particles are protons *versus* the measured time difference for events from 1200 MeV deuterons and $\vec{\mathrm{H}}$ gas (left panel) and N_2 gas (right panel) in the storage cell. These results were obtained during the January 2007 beam-time.

band of the *pp* events is very similar for $\vec{\mathrm{H}}$ and N_2 targets (and hence for the cell wall).

4.4.1 Missing–mass distributions for the $\vec{d}\vec{p} \to dp_{sp}\pi^0$ reaction

Time-of-flight cuts applied to the distributions of Fig. 6 allow us to select the *dp* candidates and hence to derive the missing–mass distributions of the $dp \to dp\pi^0$ reactions that are presented in Fig. 7 and Fig. 8. Data with the hydrogen target ($\vec{\mathrm{H}}$) show a prominent peak

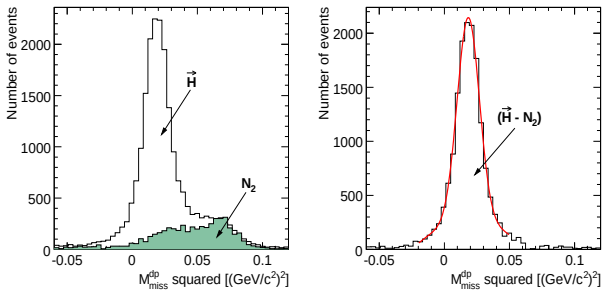

Figure 7: Missing–mass squared distribution for the reaction $\vec{d}\vec{p} \to (dp_{sp})X$ (**High** branch) measured with the storage cell and the 1200 MeV deuteron beam. The open histogram on the left panel represents the result obtained with the hydrogen gas while the shaded areas show the 'background' contributions measured with nitrogen in the cell. These latter distributions have been normalised to the hydrogen data to the right of the peak. On the right panel the data with the hydrogen target is shown after background subtraction. The missing–mass squared corresponding to the unobserved π^0 are clearly seen with the mean value of $0.0184\,(\mathrm{GeV/c^2})^2$ and $\sigma = 8.5\,(\mathrm{MeV/c^2})^2$.

corresponding to the production of a π^0. The background in both cases is very similar to that measured with the nitrogen target (N_2) and the natural assumption is that in the hydrogen case this originates from the cell walls.

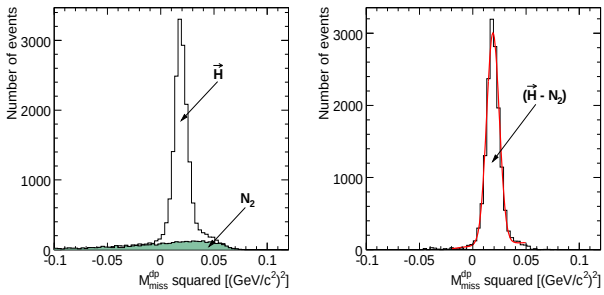

Figure 8: Missing–mass squared distribution for the reaction $\vec{d}\vec{p} \rightarrow (dp_{sp})X$ (**Low** branch) measured with the storage cell and the 1200 MeV deuteron beam. The open histogram on the left panel represents the result obtained with the hydrogen gas while the shaded areas show the 'background' contributions measured with nitrogen in the cell. These latter distributions have been normalised to the hydrogen data to the right of the peak. On the right panel the data with hydrogen target is shown after background subtraction. The missing mass squared corresponding to the unobserved π^0 are clearly seen with the mean value of $0.0189\,(\mathrm{GeV/c^2})^2$ and $\sigma = 6.0\,(\mathrm{MeV/c^2})^2$.

4.4.2 Missing–mass distribution for the $\vec{d}\vec{p} \rightarrow (pp)n$ reaction

The previous measurements with a proton beam and a hydrogen cell target [9] showed that reactions with three particles in the final state, where two of them are charged, can be identified provided that the shape of the background from the walls is known experimentally. Time-of-flight cuts applied to the distributions of Fig. 6 allow us to select the pp candidates and hence to derive the missing–mass distributions of the $dp \rightarrow (pp)n$ reaction that are presented in Fig. 9.

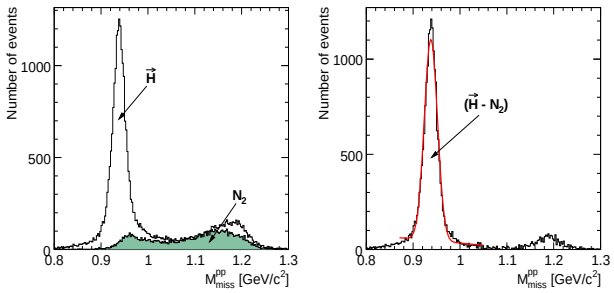

Figure 9: Missing–mass distribution for the reaction $\vec{d}\vec{p} \rightarrow (pp)X$ measured with the storage cell and the 1200 MeV deuteron beam. The open histogram on the left panel represents the result obtained with the hydrogen gas while the shaded areas show the 'background' contributions measured with nitrogen in the cell. These latter distributions have been normalised to the hydrogen data to the right of the peak. In the right panel the data with the hydrogen target is shown after background subtraction. The missing mass corresponding to the unobserved neutron is clearly seen with a mean value of $0.938\,\mathrm{GeV/c^2}$ and $\sigma = 14.0\,\mathrm{MeV/c^2}$.

4.4.3 Missing–mass distribution for the $\vec{d}\vec{p} \to {}^3\mathrm{He}\,\pi^0$ reaction

It has been shown in previous measurements at ANKE with the cluster target [7] that there is a large acceptance for the $dp \to {}^3\mathrm{He}\,\pi^0$ reaction when the ^{3}He are emitted very close to the initial beam direction. The high–momentum branch of ^{3}He particles could be selected in an off–line analysis by applying two–dimensional cuts in ΔE *versus* momentum and Δt *versus* momentum for individual layers of the forward hodoscope. The π^0 was identified through the missing mass derived from the ^{3}He measurement. After background subtraction, the mean value of the missing–mass distribution (Fig. 10) is close to the pion mass.

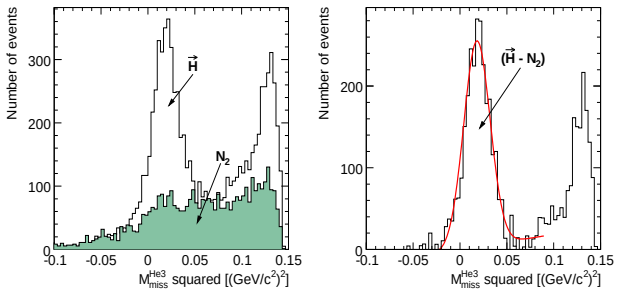

Figure 10: Missing–mass squared distribution for the reaction $\vec{d}\vec{p} \to {}^3\mathrm{He}\,X$ measured with the storage cell and the 1200 MeV deuteron beam. The open histogram on the left panel represents the result obtained with the hydrogen gas, while the shaded areas show the 'background' contributions measured with nitrogen in the cell. The latter distribution has been normalised to the hydrogen data to the right of the peak. In the right panel the data with hydrogen target is shown after background subtraction. The missing mass squared corresponding to the unobserved π^0 are clearly seen with the mean value of $0.0182\,(\mathrm{GeV/c^2})^2$ and $\sigma = 14.0\,(\mathrm{MeV/c^2})^2$.

4.4.4 STT commissioning result: identification of $\vec{d}\vec{p}$ elastic reaction

The experience gained during the PIT commissioning run in March 2006 [9], confirmed our expectation that the detection of only a single track in the forward detector would not allow us to identify unambiguously elastic scattering on hydrogen. The missing–mass spectra of Fig. 11 were deduced just from such single–deuteron events in the forward detector system. One cannot distinguish the signal ($\vec{\mathrm{H}}$ target) from the 'background' ($\mathrm{N_2}$ target), because the distributions have similar shapes with the same peak position at around proton mass. In order to identify clearly dp elastic reaction with the PIT at ANKE, it is crucial to have the STT system installed for the detection of recoil protons in coincidence with fast deuterons in the forward detector. A picture of the results with such a coincidence trigger **Forward & STT** is shown in Fig. 12. A clear proton peak from the dp elastic reaction is visible. Before we achieved this result, several intermediate steps have been tested during the STT commissioning phase (session 2), which have shown that silicon detectors:

- can be operated 5 mm close to the PIT storage cell, surviving the COSY beam–losses at injection and stacking,
- can be operated in the presence of hydrogen atoms from the ABS,
- are not affected by the H–atoms from the electron cooler,

- are not affected by the vibrations of the Cryo–pump in the ANKE target section.

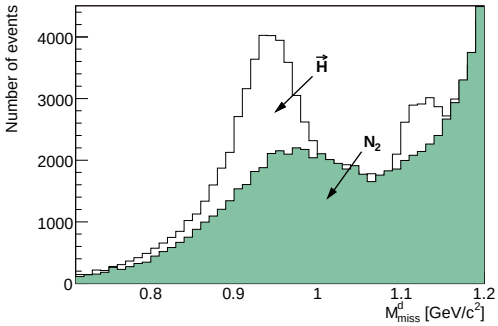

Figure 11: Missing–mass distribution for the reaction $\vec{d}\vec{p} \to dX$ measured with the storage cell and the 1200 MeV deuteron beam. The data have been taken with the **Forward** trigger alone. The open histogram represents the result obtained with the hydrogen gas while the shaded areas show the 'background' contributions measured with nitrogen in the cell. The latter distribution has been normalised to the hydrogen data to the right of the peak.

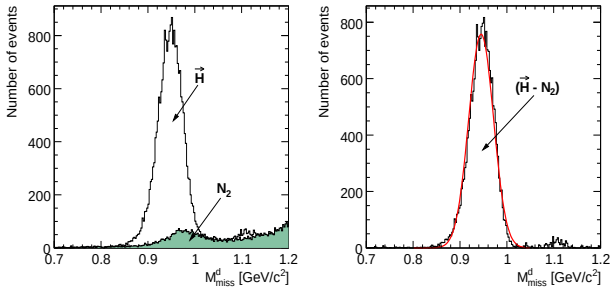

Figure 12: Missing–mass distribution for the reaction $\vec{d}\vec{p} \to dX$ measured with the storage cell and the 1200 MeV deuteron beam. The data have been taken with coincidence trigger **Forward & STT**. The open histogram in the left panel represents the result obtained with the hydrogen gas while the shaded areas show the 'background' contributions measured with nitrogen in the cell. The latter distribution has been normalised to the hydrogen data to the right of the peak. In the right panel the data with hydrogen target are shown after background subtraction. The missing mass corresponding to the unobserved proton are clearly seen with the mean value of 0.945 GeV/c^2 and $\sigma = 25.0$ MeV/c^2.

In order to prove that the operational conditions for the silicon detectors were as normal, we present below several illustrative spectra showing the performance of the STT system in the presence of the PIT.

Figure 13 shows trajectories of the particles detected in the first and the second layers (placed at $X = +20$ mm and $X = +40$ mm) of the STT and projected onto the XY–plane. Black lines in the 2-D plot show the position of the silicon detectors. The third STT layer, placed at $X = +60$ mm is not seen in this picture. The origin of the coordinate system is at the nominal central position of the cell target, in such a way that the vertical axis of the gas feeding tube is at $X = Z = 0$ and the longitudinal direction of the cell target coincides with the Z–axis. Thus the Z–axis is lying along the COSY beam towards the D2 magnet, while Y (vertical) and X (horizontal) axes are perpendicular to and in the plane of the

COSY ring, respectively. The XY–projection ($Z = 0$) shows that all trajectories have a minimum of the deviation along the Y–axis near $X = 0$ where the ABS beam position is expected.

The right panel of Fig. 13 presents the distribution of these trajectories along the Y–axis at $X = 0$. It is the projection of the left two–dimensional plot at $X = 0$. The distance between the two subsidiary peaks is about 15 mm, which coincides with the vertical dimension of the cell target ($20 \times 15 \times 390\,\mathrm{mm}^3$). In all probability, they are due to the interaction of the COSY beam halo with the cell walls.

The left panel of Fig. 14 shows the same trajectories but now projected onto the XZ–plane, while the right panel represents the distribution along the Z–axis, *i.e.*, along the cell, where the ABS gas feed tube position is expected at $Z = 0$. This is again the projection of the two–dimensional XZ plot at $Y = 0$.

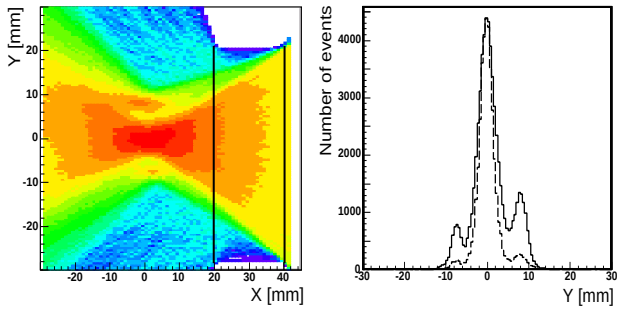

Figure 13: Left panel: two–dimensional XY–plane distribution of the particle trajectories detected in the first and the second layers of the STT system, when the proton from each event was fixed in the forward detector by the momentum cut. Black lines in the 2-D plot show the position of the silicon detectors. It is seen that all trajectories have a minimum deviations along the Y axis near $X = 0$, where the ABS atomic beam should enter the cell target. Right panel: the distribution of these trajectories along the Y–axis at $X = 0$. The interaction of a COSY beam halo with the cell walls is visible. Solid and dashed histograms stands respectively for data *without* and *with* scrapers used for the COSY beam transport through the cell. The profit achieved by using the scrapers is evident.

4.5 Polarisation determination of the hydrogen storage cell target Q_y

In this section the preliminary results on the determination of the target polarisation through the measurement of identified quasi–free $\boldsymbol{n\vec{p} \to d\pi^0}$ events, detected in the ANKE forward system, are presented.

Due to isospin invariance, the neutron analysing power in the $\vec{n}p \to d\pi^0$ reaction should be identical to that of the proton in $\vec{p}p \to d\pi^+$, for which extensive data compilations are available from SAID. As shown by our earlier measurements with a polarised deuteron beam [7], the agreement of our results with the shape of the SAID predictions is very good for both small and large deuteron cm angles. This led to a determination of the vector polarisation of the deuteron beam since, for the small Fermi momenta investigated here, there is a one–to–one relation between the deuteron and constituent neutron polarisations. The value of P_z so deduced was completely consistent with that obtained from elastic $\vec{d}p$ scattering. Within small error bars, typically 2%, there was no sign of any effect arising from the tensor polarisation of the deuteron beam.

For the new experiment in January 2007, using an unpolarised COSY deuteron beam and a polarised hydrogen storage cell target (session 1), the ϕ–dependence of the differ-

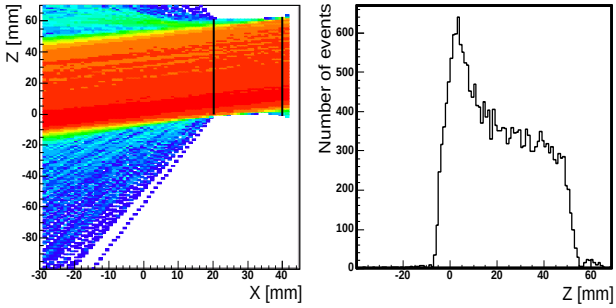

Figure 14: Left panel: two–dimensional XZ–plane distribution of the particle trajectories detected in the first and the second layers of the STT system, when the deuteron from each event was fixed in the forward detector by the momentum cut. Black lines in the 2D plot show the position of the silicon detectors. Right panel: the projection of the XZ–plane ($Y = 0$) trajectories along the Z–axis, *i.e.*, along the cell, where the ABS gas tube position is expected at $Z = 0$. The main part of this distribution in Z (cell is 390 mm long) corresponds to protons from the elastic process, which has the limited angular range due to the kinematics.

ential cross section $\sigma/\sigma_0 = 1 + Q_y\, A_y^p \cos\phi$ allowed us to extract the combination $Q_y A_y^p$. The known values of the proton analysing power A_y^p of $\vec{p}p \to d\pi^+$ then leads to the determination of the polarisation of the hydrogen target Q_y.

The Atomic Beam Source (ABS) of the ANKE polarised internal target (PIT) was operated in two spin modes: positive polarisation Q_y^+ (spin-up, WFT is **off** and MFT is **on**) and negative polarisation Q_y^- (spin-down, WFT is **on** and MFT is **on**). This has been managed by proper switching of the weak field transition (WFT) unit every 5 s **off** or **on**, while the medium field transition unit (MFT) was always switched **on**. In the following initial analysis we have assumed that $|Q_y^+| = |Q_y^-| = Q_y$, as indicated by the LSP measurements.

The event identification has been done in the following way. Figure 6 shows events from the $\boldsymbol{d\vec{p}}$ interaction sample, where two charged particles were detected in the double–layer forward scintillation hodoscope. Polarised $\vec{\mathrm{H}}$ (unpolarised N_2) gas was used in the target cell and an incident deuteron beam of 1200 MeV energy employed. The figure shows the arrival–time differences for the two particles in the hodoscope (calculated after momentum and trajectory reconstruction, under the assumption that both particles were protons) *versus* the measured difference of the two time signals from the scintillator. Thus, the two protons from the $dp \to (pp)n$ reaction should lie along the diagonal, with other pairs, such as dp_{sp} with a spectator proton from $dp \to dp_{sp}\pi^0$, being found elsewhere.

Time-of-flight cuts applied to the distributions of Fig. 6 allow us to select the dp candidates and hence to derive the missing–mass squared distributions of the $dp \to dp\pi^0$ reactions that are presented in Fig. 15. For both the high deuteron momentum part (forward production in cm system), and the low momentum region (backward production), the peaks corresponding to the unobserved π^0 are clearly seen after background subtraction using N_2 data (see Fig. 16). For small deuteron cm angles the spectrometer provides useful ϕ acceptance over the full angular range. However, for events in the backward hemisphere, this is restricted to $|\phi| < 60^\circ$.

The background–subtracted counts extracted from the different θ_{cm}^d angular intervals are listed in the Table 1 for two different spin states (N^+ and N^-). The background shape was taken from the N_2 data sample, as discussed above. Now, using the value of the asymmetry parameter $\varepsilon = (N^+ - N^-)/(N^+ + N^-)$ determined for each individual

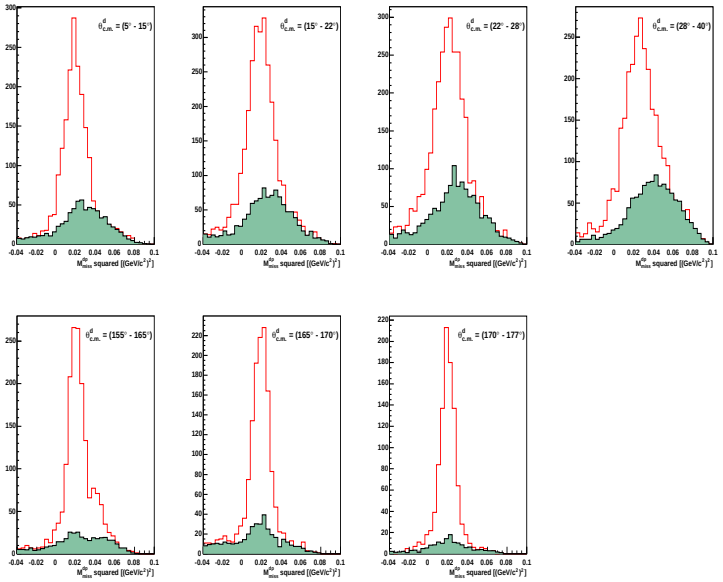

Figure 15: Angular dependence of the missing–mass squared distribution for the reaction $\boldsymbol{d\vec{p} \rightarrow (dp_{sp})X}$ (upper row **High** branch, and lower row **Low** branch) measured with the storage cell and the 1200 MeV deuteron beam. The open histogram represents the result obtained with the hydrogen gas while the shaded areas show the 'background' contributions measured with nitrogen in the cell. These results correspond to a target polarisation with 'spin-up'.

θ^d_{cm} angular bin and the values for the averaged analysing power $\langle A_y \rangle$ of protons from the SAID database, it was possible to extract the averaged target polarisation value $\langle Q_y \rangle = \varepsilon / \langle A_y \rangle \cdot \langle \cos\phi \rangle = 0.75 \pm 0.06$ with the $\chi^2/d.o.f. \approx 2/6$. (It should be noted that these results are still PRELIMINARY).

θ^d_{cm}	N^+	N^-	$\varepsilon = (N^+ - N^-)/\Sigma$	A^p_y	$\langle \cos\phi^d \rangle$	Q_y
11.2	1286.5	1030.4	0.111 ± 0.044	0.179	-0.826	-0.747 ± 0.297
19.5	1817.4	1239.4	0.189 ± 0.044	0.293	-0.860	-0.750 ± 0.173
25.8	1855.1	1045.1	0.279 ± 0.050	0.361	-0.894	-0.866 ± 0.154
32.7	1747.8	879.4	0.331 ± 0.053	0.416	-0.902	-0.881 ± 0.140
161.5	1222.6	1523.1	-0.109 ± 0.040	0.186	0.896	-0.655 ± 0.237
167.9	1095.8	1230.3	-0.058 ± 0.038	0.127	0.864	-0.526 ± 0.345
172.7	926.7	988.0	-0.032 ± 0.042	0.078	0.852	-0.483 ± 0.640

Table 1: The target polarisation Q_y extracted from the $\boldsymbol{n\vec{p} \rightarrow d\pi^0}$ reaction in the different θ^d_{cm} angular intervals.

4.5.1 Cross–check of Q_y measurements by $\boldsymbol{d\vec{p}}$ elastic reaction

At the beginning of session 3, we had several short runs with an unpolarised deuteron beam and a polarised hydrogen storage cell target. From this data sample a clean identification of the $\boldsymbol{d\vec{p}}$ elastic reaction was achieved, as demonstrated in Fig. 17. Using the known

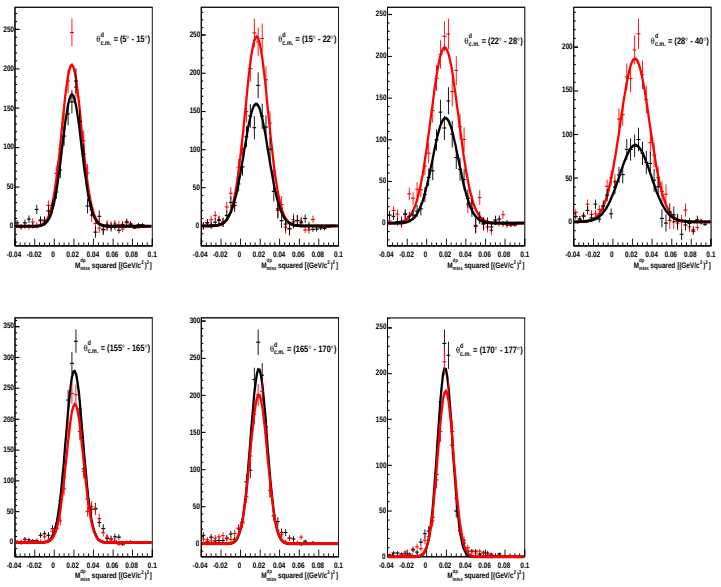

Figure 16: Angular dependence of the missing–mass squared distribution for the reaction $\boldsymbol{d\vec{p} \rightarrow (dp_{sp})X}$ (upper row **High** branch, and lower row **Low** branch) measured with the storage cell and the 1200 MeV deuteron beam. Red and black histograms stands for the data with target polarisation 'spin-up' and 'spin-down', respectively, **after background subtraction** using N_2 data.

averaged value of $\langle Q_y \rangle = 0.75 \pm 0.06$, determined from the quasi–free $\boldsymbol{n\vec{p} \rightarrow d\pi^0}$ reaction, we can extract the proton analysing power A_y^p from the dp elastic process and compare our findings to the existing results in the literature [10]. A large difference between the dp elastic counts from the 'spin-up' and 'spin-down' samples is clearly seen from the right panel of Fig. 17. The results of this investigation are listed in Table 2. The comparison of our A_y^p values at $T_d/2$=600 MeV with the published results [10] are not fully adequate because of the different energy domain, but nevertheless the results are compatible.

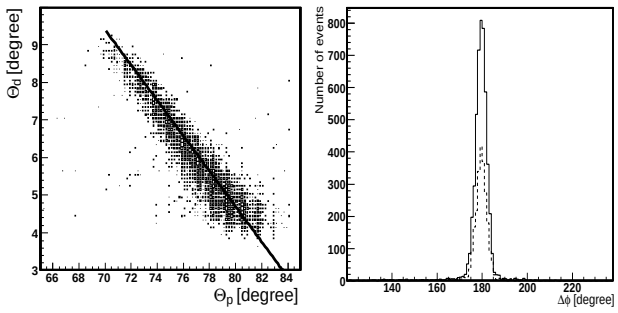

Figure 17: Left panel: angular correlation between the protons and deuterons detected in the STT and forward detector, respectively. The expected kinematical correlation for the dp elastic reaction is shown by the black line. Right panel: distribution of the azimuthal angular difference $\Delta\phi$ between the protons and deuterons from the dp elastic reaction. Solid and dashed histograms stand, respectively, for data with target polarisation 'spin-up' and 'spin-down'.

$\cos\theta^d_{cm}$	N^+	N^-	$\varepsilon = (N^+ - N^-)/\Sigma$	$\langle\cos\phi^d\rangle$	A_y^p
0.97 - 0.95	970	2003	-0.348 ± 0.017	-0.955	0.486 ± 0.037
0.95 - 0.93	699	1431	-0.344 ± 0.021	-0.975	0.470 ± 0.040
0.93 - 0.90	501	1063	-0.359 ± 0.024	-0.980	0.488 ± 0.044
0.90 - 0.85	233	462	-0.329 ± 0.039	-0.979	0.448 ± 0.059

Table 2: The angular dependence of the proton analysing power A_y^p extracted from the $\boldsymbol{d\vec{p}}$ elastic reaction assuming the target polarisation of $\langle Q_y \rangle = 0.75 \pm 0.06$.

4.6 Method to reconstruct vertex coordinate for PIT measurement

A method to reconstruct the extended target vertex coordinates was developed for the ANKE PIT commissioning beam time in November 2005, and the results are described in the IKP Annual Report [11]. The $pp \to d\pi^+$ process with the detection of both secondaries was chosen for this purpose, and a simulation has been performed to find the optimum conditions for the measurement. The $pp \to d\pi^+$ events have been identified *via* the reconstructed momenta, the arrival time difference, and the energy loss in the scintillation counters. The trajectories of both particles, together with their arrival times, allow, with the use of kinematical constraints, the reconstruction of the coordinates of the interaction point. This is accomplished by minimising the following expression:

$$\chi^2 = \sum_i \frac{(\Delta w)_i^2}{(\sigma^2 w)_i} + \mathrm{HW} \sum_{\mathrm{i}} (\Delta \mathrm{P})_{\mathrm{i}}^2 + \sum_{\mathrm{i}} \frac{(\Delta \mathrm{TOF})_{\mathrm{i}}^2}{(\sigma^2 \mathrm{TOF})_{\mathrm{i}}},$$

where the first term includes the deviations of the trajectories in the MWPCs, the second one is the kinematical term, applied with a 'heavy weight' HW. ΔTOF was calculated as $\Delta\mathrm{TOF} = \tau(\vec{\mathrm{p}}, \mathrm{l}, \mathrm{m}) - \mathrm{TDC}\cdot\mathrm{channel}$, where $\tau(p, l, m)$ is the TOF from the vertex, calculated from the particle momentum, trajectory length and the assumed mass, and TDC·channel is the measured arrival time. This procedure provides a measurement of the gas density distribution inside the cell and a separation of the background $d\pi^+$ pairs originating from the rest gas in the target and magnet chambers. Appropriate software for the vertex reconstruction has been developed.

The method was tested during a beam time in November 2005 [11]. A calibration run with a point–like CH_2 strip target allowed us to tune the $d\pi^+$ event separation and confirmed that the obtained detector acceptance corresponds to the simulated one. In the left panel of Fig. 18 the comparison of the measured arrival time difference with the one calculated for pion and deuteron masses is shown for the storage cell data. The large ΔTOF of $d\pi^+$ pairs allows us to identify them practically without dilution from pairs of other particles.

The distribution of coordinates obtained with the storage cell (right panel of Fig. 18), shows the events produced inside the cell as well as the background. The origin in the figure corresponds to the ABS jet position and the X and Y coordinates follow the positions of the COSY beam. The data show that the resolution of the reconstructed vertex coordinate is $\sigma_Z = 3.6\,\mathrm{cm}$ longitudinally and $\sigma_X = 0.8\,\mathrm{cm}$ transversely.

The same method has been applied to the current data and preliminary results will be presented during PAC session.

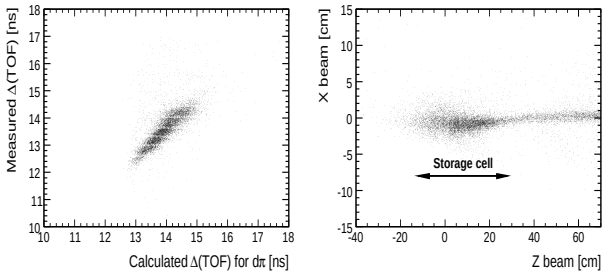

Figure 18: Left panel: identification of $d\pi^+$ events by TOF information. Right panel: reconstructed vertex coordinates for the cell measurement (data from PIT commissioning beam time in November 2005).

4.7 Deuteron beam polarisation determination from $\vec{n}p \to d\pi^0$ (P_z)

For the current measurements in January 2007 we have used the polarised deuteron beam from the COSY ion source. The actual scheme consisted of five different polarisation states, one unpolarised state and four combinations of vector and tensor polarisation, as shown in Table 3.

	theoretical maximum			
Mode	vector P_z	tensor P_{zz}	Intensity I_0	P_z^{LEP}
1	0	0	1	$+0.008 \pm 0.008$
2	$-2/3$	0	1	-0.545 ± 0.006
3	$+1/3$	-1	1	$+0.257 \pm 0.008$
4	-1	$+1$	$2/3$	-0.723 ± 0.006
5	$+1$	$+1$	$2/3$	$+0.597 \pm 0.004$

Table 3: The table lists the five configurations of the polarised deuteron ion source, showing the ideal values of the vector (P_z) and tensor polarisations (P_{zz}) and the relative beam intensities obtained by operating the three radio–frequency transitions. Also shown are the measured vector polarisations of the deuteron beam with statistical errors. The determinations of P_z^{LEP} were carried out at a deuteron momentum of 539 MeV/c using the Low Energy Polarimeter (LEP). The averaged over all spin modes ANKE value $\langle P_z^{ANKE} \rangle = 0.60 \pm 0.10$ were obtained assuming that state–0 was unpolarised. The quoted result is compatible with the average value of $\langle P_z^{LEP} \rangle = 0.660 \pm 0.003$, obtained from the LEP measurements. It should be noted that these results are still PRELIMINARY.

As already mentioned, in the second beam-time session, during two days of measurements, the data were taken with a polarised deuteron beam and unpolarised H_2 target from the Unpolarised Gas Supply System with the calibrated flux into the cell. The goal was to determine the vector polarisation (P_z) of the deuteron beam from the same quasi–free $\vec{n}p \to d\pi^0$ reaction. The procedure is the same as that used for the determination of the target polarisation. The results achieved are given in Table 3.

4.8 Deuteron beam polarisation determination from $\vec{d}\vec{p}$ elastic (P_z, P_{zz})

Analysis is in progress !
Preliminary results will be presented during the PAC session in May.

4.9 Beam and Target polarimetry

Analysis is in progress !
Preliminary results will be presented during the PAC session in May.

5 Requested Beam Time

- The **proposal requires a TOTAL of four weeks** to determine the vector $C_{y,y}(C_{x,x})$ and tensor $C_{yy,y}$ spin–correlation coefficients at two energies $T_d = 1.2\,\mathrm{GeV}$ and $T_d = 2.23\,\mathrm{GeV}$.
- With the **PRESENT request** the collaboration asks for the allocation of **four weeks** of beam time to complete the proposed experiment after the re-installation of the PIT at ANKE.

References

[1] A. Kacharava, F. Rathmann, and C. Wilkin for the ANKE Collaboration, COSY Proposal #172 (2006); http://www.fz-juelich.de/ikp/anke/proposals.shtml.

[2] F. Rathmann, for the ANKE Collaboration, COSY Proposal #146 (2006); http://www.fz-juelich.de/ikp/anke/proposals.shtml.

[3] R. Schleichert, for the ANKE Collaboration, COSY Proposal #159 (2006); http://www.fz-juelich.de/ikp/anke/proposals.shtml.

[4] A. Roth, Vacuum Technology, Elsevier Science B.V., (1990) 84.

[5] R. Engels *et al.*, Rev. Sci. Instr. **74** (2003) 4607.

[6] R. Engels *et al.*, Rev. Sci. Instr. **76** (2005) 053305.

[7] D. Chiladze *et al.*, Phys. Rev. ST Accel. Beams, **9** (2006) 050101.

[8] W. Haeberli et al., Phys. Rev C **55** (1997) 597; F. Rathmann et al., Phys. Rev C **58** (1998) 658, H.O. Meyer et al., Phys. Rev C **63** (2001) 064002.

[9] L. Barion *et al.*, Status Report for Experiment #146.1, (May 2006), available from http://www.fz-juelich.de/ikp/anke/proposals.shtml.

[10] E. Winkelmann *et al.*, Phys. Rev. C **21** (1980) 2535.

[11] S. Dymov *et al.*, IKP Annual Report 2005, available from http://www.fz-juelich.de/ikp/anke/Annual-Report-05.shtml.